creative commons
COMMONS DEED

저작자표시-비영리-변경금지 2.0 대한민국

이용자는 아래의 조건을 따르는 경우에 한하여 자유롭게

- 이 저작물을 복제, 배포, 전송, 전시, 공연 및 방송할 수 있습니다.

다음과 같은 조건을 따라야 합니다:

저작자표시. 귀하는 원저작자를 표시하여야 합니다.

비영리. 귀하는 이 저작물을 영리 목적으로 이용할 수 없습니다.

변경금지. 귀하는 이 저작물을 개작, 변형 또는 가공할 수 없습니다.

- 귀하는, 이 저작물의 재이용이나 배포의 경우, 이 저작물에 적용된 이용허락조건을 명확하게 나타내어야 합니다.
- 저작권자로부터 별도의 허가를 받으면 이러한 조건들은 적용되지 않습니다.

저작권법에 따른 이용자의 권리는 위의 내용에 의하여 영향을 받지 않습니다.

이것은 이용허락규약(Legal Code)을 이해하기 쉽게 요약한 것입니다.

Disclaimer

dCollection

조선대학교
CHOSUN UNIVERSITY

February 2023

Master's Degree Thesis

A Study on the Prediction Model of Propagation Path Loss for 5G Frequency Band

Graduate School of Chosun University

Department of Information and Communication Engineering

Hyeong-Jung Kim

조선대학교
CHOSUN UNIVERSITY

A Study on the Prediction Model of Propagation Path Loss for 5G Frequency Band

5G 주파수 대역의
전파경로손실 예측 모델에 대한 연구

February 24, 2023

Graduate School of Chosun University

Department of Information and Communication Engineering

Hyeong-Jung Kim

조선대학교
CHOSUN UNIVERSITY

A Study on the Prediction Model of Propagation Path Loss for 5G Frequency Band

Advisor: Prof. Dong-You Choi

This thesis is submitted to the Graduate School of Chosun University in partial fulfillment of the requirements for the Master's degree engineering.

October 2022

Graduate School of Chosun University

Department of Information and Communication Engineering

Hyeong-Jung Kim

조선대학교
CHOSUN UNIVERSITY

This is to certify that the Master's thesis of

Hyeong-Jung Kim

has been approved by the examining committee for the thesis requirement for the Master's degree in engineering

Committee Chairperson
Chosun University **Prof. Goo-Rak Kwon (Sign)**

Committee Member
Chosun University **Prof. Sun-Kuk Noh (Sign)**

Committee Member
Chosun University **Prof. Dong-You Choi (Sign)**

December 2022

Graduate School of Chosun University

조선대학교
CHOSUN UNIVERSITY

Table of Contents

조선대학교
CHOSUN UNIVERSITY

조선대학교
CHOSUN UNIVERSITY

조선대학교
CHOSUN UNIVERSITY

List of Tables

조선대학교
CHOSUN UNIVERSITY

조선대학교
CHOSUN UNIVERSITY

List of Figures

조선대학교
CHOSUN UNIVERSITY

요 약

5G 주파수 대역의
전파경로손실 예측 모델에 대한 연구

김 형 중

지도교수: 최 동 유

조선대학교 대학원 정보통신공학과

최근에 모바일 데이터 트래픽의 기하급수적인 증가와 더 높은 전송속도에 대한 수요가 계속 증가함으로써 보다 정확하고 간단한 전파경로손실 예측이 필요하다. 5G 시스템의 주파수 대역인 3.7 GHz 와 28 GHz 대역에서 8가지의 다양한 전파환경(보통 길이의 복도, 긴 길이의 복도, 원형 복도, 터널, 작은 사이즈 강당, 큰 사이즈 강당, 개방형 10층 계단, 폐쇄형 6층 계단)에 대하여 4개의 잘 알려진 모델(CI (Close-In), CIF (CI model with a frequency-weighted path loss exponent), FI (Floating-Intercept), and ABG (Alpha-Beta-Gamma))을 활용하여 단일 및 다중 주파수 통계 모델에 대한 전파 특성을 측정 및 분석한다.

측정 결과는 FI 모델이 다양한 전파환경에서 실제 측정값과 예측값이 비교적 유사한 결과를 보이며, CIF 모델은 실제 측정값과 예측값이 차이가 있음을 확인할 수 있다.

조선대학교
CHOSUN UNIVERSITY

Ⅰ. Introduction

The conflict between capacity growth and insufficient frequency bands has become highly important with the exponential growth of mobile data traffic and the demand for higher transmission rates. Thus, accurate and simple models for predicting propagation path loss are important because mobile broadband networks should satisfy consumers' demand for higher data rates and require stronger wireless access technologies that can reliably operate in high frequency bands to address the requirements of wireless operators [1].

The mmWave frequencies encounter many challenges such as multiple path loss and high penetration loss. Therefore, reliable channel propagation characteristics (a model) are required for accurate and convenient indoor communication systems. Similarly, further research is required on the characteristics of mmWave for 5G systems. In the many literature, 5G system bands have been compared in various environments [2-6].

Because optimal network planning for wireless communication systems requires an adequate knowledge of the channel characteristic of the target coverage, it is feasible to estimate the channel parameters through comprehensive measurements in various environments [7].

The indoor environment differs from the outdoor environment in various aspects. The floor plans, building materials used, human movements, and transitions in the nearby devices should be considered for indoor models. The properties of the received signal are also impacted by general fading and path loss caused by distance, interference, reflection, scattering, and penetration [8]. The propagation path loss prediction model is essential for understanding the attenuation of propagation. Therefore, this study measured the propagation path loss based on the average received power in eight measurement environments (normal corridor, long corridor, tunnel, circular corridor, small auditorium, large auditorium, open staircase, and closed staircase).

Propagation path loss modeling and channel characterization have been analyzed

조선대학교
CHOSUN UNIVERSITY

based on well-known single-frequency and multi-frequency band propagation prediction models and directivity and omnidirectional prediction models [9].

In this study, propagation path loss was analyzed based on the measurement data in the 5G system frequency bands of 3.7 GHz and 28 GHz. Accordingly, Chapter 2 describes the radio wave path loss prediction model. Various radio wave measurement environments are discussed in Chapter 3. Chapter 4 analyzes the predicted value of radio wave path loss based on the measured value. Chapter 5 draws conclusions based on the research results.

조선대학교
CHOSUN UNIVERSITY

Ⅱ. Propagation Path Loss Model

A. The Need for a Propagation Path Loss Model

Propagation path loss is a decrease in undesired signal intensity that occurs when a radio signal is propagated between a transmission antenna and reception antenna. The prediction accuracy and simplicity of the model are key concerns for the performance of the propagation path loss prediction model. These should be developed further for 5G systems and beyond [10].

$$PL = P_{Tx} - P_{Rx} + G_{Tx} + G_{Rx} - C_{Tx} - C_{Rx}, \tag{2.1}$$

where PL is the path loss, P_{Tx} is the transmitted power at Tx, P_{Rx} is the received power at Rx, G_{Tx} is the antenna gain of Tx, G_{Rx} is the antenna gain of Rx, C_{Tx} is the cable loss of Tx, and C_{Rx} is the cable loss of Rx.

In general, the direct propagation path loss for each position of Rx can be obtained as shown in Equation (2.1) [11].

Radio waves transmitted from a transmitter to a receiver interact with surrounding obstacles. The results in reflection, diffraction, and scattering. This phenomenon causes multipath fading at the receiver's location, and the signal strength transmitted decreases as the distance increases [12].

The propagation model was initiated by Friis in 1946. It was the first development of the propagation path loss model. The model was developed based on the electromagnetic properties of the ideal state. An advantage of the Friis model is the minimal loss in the computational process. However, its disadvantage is its low accuracy. The basic formula for predicting the received signal strength under the line of sight (LOS) condition between isotropic antennas in free space is shown in Equation (2.2):

조선대학교
CHOSUN UNIVERSITY

$$\frac{P_{Rx}}{P_{Tx}} = \frac{A_{Rx}A_{Tx}}{d^2\lambda^2}, \tag{2.2}$$

where A_{Rx} is the effective area of the receiving antenna, A_{Tx} is the effective area of the transmitting antenna, d is the distance between the transmitter and receiver, and λ is the wavelength of the carrier wave.

Flexible path loss exponent: It can be defined as a function of the square of distance between the transmitter and receiver. In general, α is set to two. However, a larger value is used in the non-line of sight (NLOS) environment [13].

$$P_{Rx} = P_{Tx} - (10\alpha\log\frac{d}{d_0} + 20\log(f) + 32.45). \tag{2.3}$$

The wave propagation path loss may be estimated accurately if detailed prior knowledge of the terrain is available. Thus, these models have been developed by systematically interpreting the obtained measurement data. The Egli and Hata models are included in the empirical model [13].

Egli : It is a model proposed by John Egli in 1975, which was measured and developed in New York and New Jersey. The simplified equation is shown in Equation (2.4):

$$\begin{aligned} P_{Rx} &= P_{Tx} - 20\log(f) + 40\log(d)20\log(h_{Tx}) + k, \\ k &= \begin{cases} 76.3 - 10\log(h_{Rx}), h_{Rx} \le 10 \\ 85.9 - 20\log(h_{Rx)}, \ h_{Rx} \ge 10 \end{cases}, \end{aligned} \tag{2.4}$$

where $h_{Tx}$is the height of Tx and h_{Rx} is the height of Rx.

Hata : It is an empirical model based on the measurement results obtained by Okumura in the urban area of Tokyo. It is shown in Equation (2.5):

조선대학교
CHOSUN UNIVERSITY

$$L_{50}(urban)\,[dB] = 69.55 + 26.16\log(f_c) - 13.82\log(h_{te}) - a(h_{re}) + (44.9 - 6.55\log(h_{te}))\log(d), \quad (2.5)$$

where f_c is the frequency (150 MHz～1500 MHz), h_{te} is the height of the transmitter (30 m～200 m), and h_{re} is the height of the receiver (1 m～10 m).

Since the previous decade, many types of empirical models have been developed to support 5G mmWave networks such as 3GPP and NYUSIM. Many researchers have developed different types of propagation path loss models to predict propagation path loss. This is because the propagation path loss is likely to be misinterpreted if the model is applied to other environments. This trend may result in the development of mmWave propagation path loss prediction models as a key support solution for 5G wireless networks and beyond.

B. CI Model

CI models have been used for decades to account for propagation path loss and relative path loss at close free-space reference distances from the perspective of transmitters. The CI model is a statistical and probabilistic model that explains the large-scale propagation path loss owing to distance at different frequencies for a specific scenario. The main advantage of using the CI model is that it relies on one parameter (namely, the path loss exponent (PLE, n)) in conjunction with the standard deviation of shadow fading (SF) that reflects the fluctuations of the radio signal owing to obstacles. A single-parameter CI model enables a stable prediction of propagation path loss beyond the measured area and direct comparisons across frequency bands and environments and scenarios through simple calculations without loss of accuracy [14]. The PLE value for all frequencies is lower than or higher than the PLE value of the theoretical free space of two. This indicates that the multipath component (MPC) was summed up on the wall of the corridor and attained Rx. Thereby, when the PLE value is low, signal power attenuation becomes low as the Tx-Rx separation distance

조선대학교
CHOSUN UNIVERSITY

increases [9][14][15][18][20].

The predicted value of propagation path loss considering PLE and SF is shown in Equation (2.6):

$$PL_{(f,d)}^{CI}[dB] = FSPL[dB] + 10n\log(d) + X_{\sigma}^{CI}, \tag{2.6}$$

where n is the PLE; d is the distance between the transmitter and receiver; and d_0 is the reference distance in free space. X_{σ}^{CI} is the loss owing to reflection, scattering, diffraction, etc. It is a gaussian random variable (GRV) with a standard deviation of σ and mean of zero.

The CI model essentially implies the inclusion of dependencies on the frequency of path loss contained in the free space path loss (FSPL). The FSPL in Equation (2.6) is expressed as shown in Equation (2.7):

$$FSPL[dB] = 20\log(\frac{4\pi f d_0}{c}) = 32.4 + 20\log(f), \tag{2.7}$$

where c is the speed of light.

The PLE is determined by the minimum mean square error (MMSE) method. Assuming $A = PL_{(f,d)}^{CI} - FSPL$ and $B = 10\log_{10}(d)$ to determine the PLE value for optimal propagation path loss, the PLE value can be defined as shown in Equation (2.8):

$$n = \frac{\Sigma AB}{\Sigma B^2}. \tag{2.8}$$

The minimum standard deviation of SF is defined as shown in Equation (2.9):

$$\sigma_{\min}^{CI} = \sqrt{\frac{\Sigma(A - nB)^2}{N}}, \tag{2.9}$$

where N is the number of measured data.

조선대학교
CHOSUN UNIVERSITY

C. CIF Model

A frequency-dependent loss occurs when Rx is at a distance of over 1 m from Tx, owing to its surroundings. Therefore, it can be considered suitable for multi-frequency schemes in closed indoor environments. The CIF model is a frequency-weighted model using FSPL for a reference distance of 1 m (identical to the CI model). Therefore, it is proposed to model the radio path loss of indoor channels for 5G systems as mmWave owing to multiple frequencies [14-18].

$$PL_{(f,d)}^{CIF}[dB] = FSPL[dB] + 10n\log(\frac{d}{d_0})\ (1 + b\,(\frac{f - f_0}{f_0})) + X_\sigma^{CIF}, \qquad (2.10)$$

where n is dependent on the distance of path loss and is similar to PLE. b is a suitable parameter for the model that can verify the dependence on the linear frequency of path loss. X_σ^{CIF} is a GRV with a standard deviation for the CIF model and a mean of zero. f_0 is the average of the weighted frequencies of all the measurements for each environment and scenario, the sum of the frequency and the number of measurements in a particular frequency and scenario multiplied by the total number of measurements performed for all the frequencies. This is shown in Equation (2.11):

$$f_0 = \frac{\sum_{k=1}^{k} f_k N_k}{\sum_{k=1}^{k} N_k}, \qquad (2.11)$$

where k is the number of measured frequency bands. N_k is the number of measurements of path loss data corresponding to f_k [16][17].

It is assumed that $A = PL_{(f,d)}^{CIF} - FSPL$, $B = 10\log(\frac{d}{d0})$, $x = n\ (1-n)$, and $y = \frac{nb}{f_0}$. These are shown in Equation (2.12):

조선대학교
CHOSUN UNIVERSITY

$$X_{\sigma}^{CIF} = A - B\,(x + yf)\,. \tag{2.12}$$

The standard deviation of SF is shown in Equation (2.13):

$$\sigma^{CIF} = (\Sigma X_{\sigma}^{CIF}/N)\,. \tag{2.13}$$

To minimize the standard deviation in Equation (2.13), x and y should be zero. Their simplified forms are shown in Equations (2.14) and (2.15):

$$x = \frac{\Sigma B^2 f \Sigma BAF - \Sigma B^2 f^2 \Sigma BA}{(\Sigma B^2 f)^2 - \Sigma B^2 \Sigma B^2 f^2}\,, \tag{2.14}$$

$$y = \frac{\Sigma B^2 f \Sigma BA - \Sigma B^2 \Sigma BAf}{(\Sigma B^2 f)^2 - \Sigma B^2 \Sigma B^2 f^2}\,. \tag{2.15}$$

The minimum standard deviation of the CIF model can be obtained by substituting the x and y of Equations (2.14) and (2.15) into Equation (2.16). In addition, n and b can be calculated by substituting Equations (2.14) and (2.15) into $x = n(1-n)$ and $y = \frac{nb}{f_0}$:

$$\sigma_{\min}^{CIF} \equiv \sqrt{\frac{\Sigma (A - B(x + yf))^2}{N}}\,. \tag{2.16}$$

D. FI Model

The CI model uses only one parameter : PLE. However, the FI model requires two parameters [7]. Unlike the CI model, the FI model does not consider the physical reference distance. Thereby, it can more accurately predict radio path loss in a specific environment. Based on the MMSE method, the FI model determines the curves most

조선대학교
CHOSUN UNIVERSITY

similar to the actual measurement data and transforms these into two parameters : slopes and intercepts. This is shown in Equation (2.17) [9][14][15][19]:

$$PL_{(d)}^{FI}[dB] = \alpha + 10\beta \log(d) + X_{\sigma}^{FI}, \tag{2.17}$$

where α is the floating-intercept in dB and β is the slope of the FI model. A slope similar to that of the PLE. X_{σ}^{FI} is a GRV with a mean of zero. σ is the standard deviation that defines the large signal variation for the average propagation path loss over the length between the transmitter and receiver.

Assuming that $A = PL_{(d)}^{FI}$ and $B = 10\log_{10}(d)$ in Equation (2.17), the two variables α and β can be obtained as shown in Equations (2.18) and (2.19) to minimize σ:

$$\alpha = \frac{\Sigma B \Sigma BA - \Sigma B^2 \Sigma A}{(\Sigma B)^2 - N\Sigma B^2}, \tag{2.18}$$

$$\beta = \frac{\Sigma B \Sigma A - N\Sigma BA}{(\Sigma B)^2 - N\Sigma B^2}. \tag{2.19}$$

Because the floating-intercept is modeled as a variable, FI models can generally obtain smaller σ compared with CI models, based on identical measurement data. The minimum standard deviation of the FI model is shown in Equation (2.20):

$$\sigma_{\min}^{FI} = \sqrt{\frac{(A - \alpha - \beta B)^2}{N}}. \tag{2.20}$$

조선대학교
CHOSUN UNIVERSITY

E. ABG Model

The propagation path loss is measured in different bands. Thereby, it is feasible to investigate propagation path loss in various bands using a multi-frequency path loss model [14][15][18][20].

The ABG model may be applied through three parameters: α, β, and γ. This is shown in Equation (2.21):

$$PL_{(f,d)}^{ABG}[dB] = 10\alpha \log(\frac{d}{d_0}) + \beta + 10\gamma \log(\frac{f}{1GHz}) + X_\sigma^{ABG}, \tag{2.21}$$

where α and γ are coefficients that explain the dependence of distance and frequency on path loss, β is the offset value optimized in path loss, and X_σ^{ABG} is a GRV with a mean of zero. γ is the standard deviation that defines the large signal variation for the mean path loss for the length between the transmitter and receiver. The ABG model is an extension of the FI model at multiple frequencies, because it is similar to the FI model when γ is zero or two.

Equation (2.21) becomes identical to Equation (2.22) when it is assumed that $A = PL_{(f,d)}^{ABG}$, $B = 10\log_{10}(d)$, and $C = 10\log_{10}(f)$:

$$X_\sigma^{ABG} = A - \alpha B - \beta - \gamma C. \tag{2.22}$$

The standard deviation of SF is shown in Equation (2.23):

$$\sigma^{ABG} = \sqrt{\frac{\Sigma X_\sigma^{ABG^2}}{N}}. \tag{2.23}$$

$\Sigma X_\sigma^{ABG^2}$ can be calculated by making 0 as shown in Equation (2.24) to obtain the minimized σ^{ABG}:

조선대학교
CHOSUN UNIVERSITY

$$\begin{cases} \alpha\Sigma B^2+\beta\Sigma B+\gamma\Sigma BC-\Sigma BA=0 \\ \alpha\Sigma B+N\beta+\gamma\Sigma C-\Sigma A=0 \\ \alpha\Sigma BC+\beta\Sigma C+\gamma\Sigma C^2-\Sigma C=0, \end{cases}$$

$$\begin{pmatrix}\alpha\\ \beta\\ \gamma\end{pmatrix}=\begin{pmatrix}\Sigma B^2 & \Sigma B & \Sigma BC\\ \Sigma B & N & \Sigma C\\ \Sigma BC & \Sigma C & \Sigma C^2\end{pmatrix}^{-1}\begin{pmatrix}\Sigma BA\\ \Sigma A\\ \Sigma CA\end{pmatrix}. \tag{2.24}$$

The minimum standard deviation of SF can be obtained using Equation (2.24) with α, β, and γ. This is shown in Equation (2.25):

$$\sigma_{\min}^{ABG}=\sqrt{\frac{\Sigma(A-\alpha\beta-\beta-\gamma C)^2}{N}}. \tag{2.25}$$

조선대학교
CHOSUN UNIVERSITY

Ⅲ. Propagation Path Loss Measurement Environment

A. Measurement Equipment

The M5183B keysight signal generator, and PXI 9393A signal analyzer were used in this study. The antennas used for the measurements were directional horn antennas, an omnidirectional antenna (ODA), and a tracking and standard gain horn antenna (TAS). The complete measurement setup is shown in Figure 3.1.

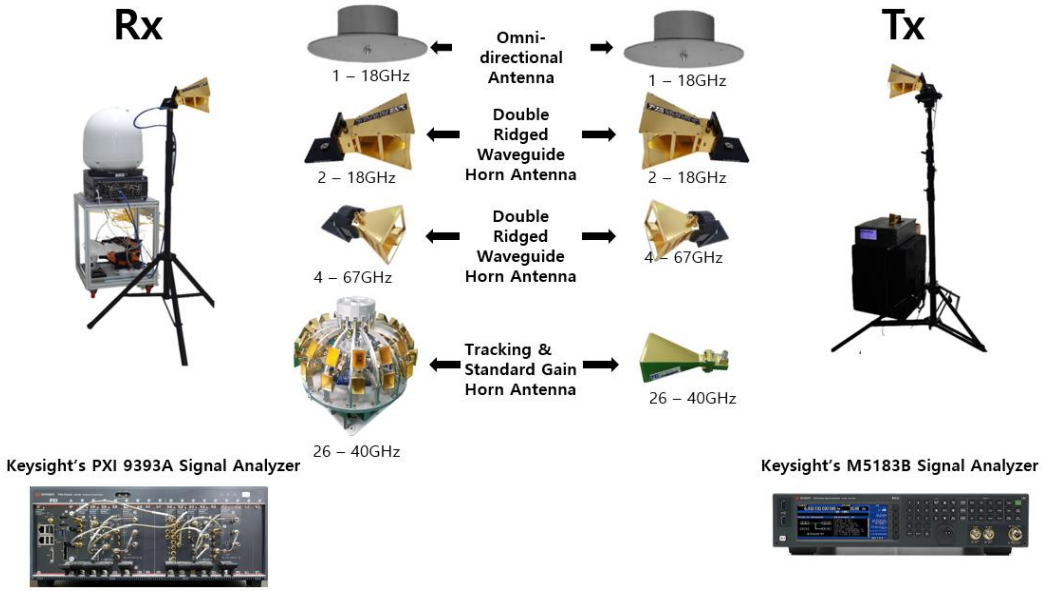

Figure 3.1. Measurement system

A directional horn antenna of 3.7 GHz and 28 GHz, directional horn antenna of 3.7 GHz and a TAS of 28 GHz were used as H-H co-polarization. The specifications of the antennas used are shown in Table 3.1. The cable losses used at 3.7 GHz and 28 GHz are －2.8 dB and －9.4 dB, respectively.

조선대학교
CHOSUN UNIVERSITY

Table 3.1. Specifications of the used antennas

Antenna	Frequency Range [GHz]	Gain [dBi]	Beamwidth (3dB, V)	Beamwidth (3dB, H)
ODA0467-10	1～18	0	-	-
BWA0218-10	2～18	10	45°	40°
BWA0467-10	4～67	10	45°	40°
WR28-20A	26.5～40	20	20°	18°

B. Measurement Scenario

1. Scenario (1) : Normal Corridor

The first scenario was measured in the corridor on the 10th floor of Chosun University's IT Convergence University in Gwangju. As shown in Figure 3.2, the material of the corridor (which has a width, length, and height of approximately 2.6 m, 100 m, and 2.7 m, respectively) is designed with walls made of plywood and concrete, iron doors, glass, and square tile floors. At a distance of 50 m from Tx, it consists of men's and women's restrooms, an elevator, a staircase leading down to the lower floor, and an empty space. Tx had a height of 1.75 m, The height of Rx was set to 1.5 m, which is the average height when a mobile device is lifted. Rx was moved from Tx by 10 m. The measurements were performed as shown in Table 3.2 in a closed environment where all the doors were closed and all the lights in the corridor were switched off at nine points.

조선대학교
CHOSUN UNIVERSITY

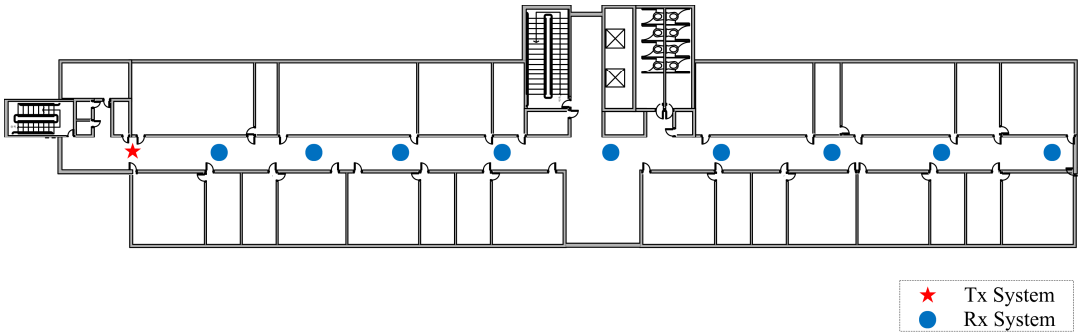

Figure 3.2. Floor plan of a normal corridor

Table 3.2. Key parameters for measurement in scenario (1)

Frequency [GHz]	Antenna	SG Power [dB]	Cable Loss [dB]	Antenna Gain [dB]	Power [dB]
3.7	Horn	0	2.8	10	7.2
28	Horn	0	9.4	20	10.6
	TAS				

2. Scenario (2) : Long Corridor

In the second scenario, the measurements were performed in the corridor on the third floor of the main building (see Figure 3.3). The main building has a length, width, and height of 375 m, 2.9 m, and 3.43 m, respectively. It is the longest building in the East to be listed in the Guinness Book of Records. It consists of a material identical to that in Scenario (1), with exterior/inner staircases at both ends and in the middle. As shown in scenario (1), the height of Tx was 1.75 m and the average height of Rx was set to 1.5 m when the mobile device was lifted. Rx moved with all the classroom doors closed and all the lights switched off, every 10 m from Tx to 100 m and every 20 m after 100 m. Measurements were performed at 18 points as shown in Table 3.3.

조선대학교
CHOSUN UNIVERSITY

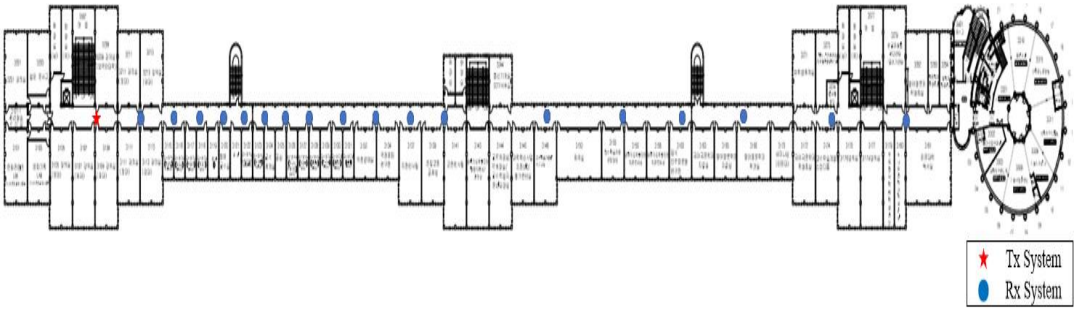

Figure 3.3. Floor plan of a long corridor

Table 3.3. Key parameters for measurement in scenario (2)

Frequency [GHz]	Antenna	SG Power [dB]	Cable Loss [dB]	Antenna Gain [dB]	Power [dB]
3.7	Horn	0	2.8	10	7.2
28	Horn	0	9.4	20	10.6

3. Scenario (3) : Circular Corridor

In the third scenario, measurements were performed in the circular building of the College of Fine Arts and Sports. The total circumference, width, and height are 83 m, 6 m, and 2.6 m, respectively (see Figure 3.4). It is made of material identical to that in scenario (1). Five square pillars with a length, width, and height of 1 m, 1 m, and 2.6 m, respectively, are arranged in front of the elevator. There are staircase in the opposite direction of the elevator. Measurements were performed as shown in Table 3.4 assuming that Tx, P1, P2, and P3 are at the 12 o'clock, 9 o'clock, 6 o'clock, and 3 o'clock positions of a clock.

조선대학교
CHOSUN UNIVERSITY

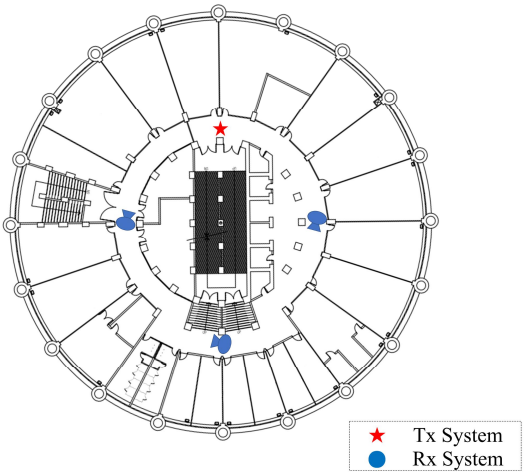

Figure 3.4. Floor plan of a circular corridor

Table 3.4. Key parameters for measurement in scenario (3)

Frequency [GHz]	Antenna	SG Power [dB]	Cable Loss [dB]	Antenna Gain [dB]	Power [dB]
3.7	Horn	0	2.8	10	7.2
28	Horn	0	9.4	20	10.6
	TAS				

4. Scenario (4) : Tunnel

In the fourth scenario, measurements were acquired immediately before the completion of the newly constructed tunnel for train cargo transportation in Mangyang-ri, Giseong-myeon, Uljin-gun, Gyeongsangbuk-do. The tunnel has a length, width, and height of 1,674 m, 3.3 m, and 4.8 m, respectively. As illustrated in Figure 3.5, Rx was positioned at a height of 1.5 m from the rail considering the location of a mobile device when an individual sits. Tx was positioned at a height of 2 m. Rx was

조선대학교
CHOSUN UNIVERSITY

shifted 10 m from the tunnel entrance to perform measurements as shown in Table 3.5. There are irregular spaces used as emergency exits or emergency passages in each middle of the tunnel.

Figure 3.5. Tx and Rx in a tunnel

Table 3.5. Key parameters for measurement in scenario (4)

Frequency [GHz]	Antenna	SG Power [dB]	Cable Loss [dB]	Antenna Gain [dB]	Power [dB]
3.7	Horn	20	2.3	10	27.7
28	Horn	20	6.5	20	33.5
	TAS				

5. Scenario (5) : Small Auditorium

In the fifth scenario, measurements were performed at three points in the IT hall located on the third floor of Chosun University's IT Convergence University (see Figure 3.6). The hall can accommodate 288 individuals. P1 and P3 were approximately 1.3 m

조선대학교
CHOSUN UNIVERSITY

apart from the walls on both sides. In the case of P2, owing to the reflection of the beam projector structure immediately above Rx, it was spaced 1.5 m from the wall behind and measured as shown in Table 3.6. The distances of Tx and Rx were 21.5 m, 20.5 m, and 21.5 m in the order of points, respectively.

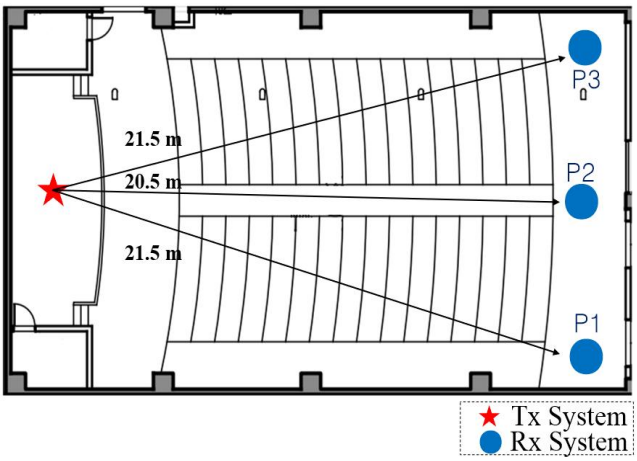

Figure 3.6. Floor plan of a small auditorium

Table 3.6. Key parameters for measurement in scenario (5)

Frequency [GHz]	Antenna	SG Power [dB]	Cable Loss [dB]	Antenna Gain [dB]	Power [dB]
3.7	Horn	0	2.8	10	7.2
	ODA				
28	Horn	0	9.4	20	10.6
	TAS				

6. Scenario (6) : Large Auditorium

In the sixth scenario, measurements were performed at the Haeoreumgwan Hall of Chosun University. The hall can accommodate approximately 1,000 individuals. As

조선대학교
CHOSUN UNIVERSITY

shown in Figure 3.7, there are two staircases to the left and right between the second and third floors to the entrance. Behind the rostrum where the Tx was installed, a large empty space is covered by curtains. The distances between Tx and Rx were 25.5 m, 23 m, 25.5 m, 37.5 m, 36 m, and 37.5 m in the order of points, respectively. The measurement points on the second floor were approximately 13 m apart, those on the third floor were approximately 14 m apart. Unlike scenario (5), additional Tx-side directional horn antennas at 3.7 GHz and 28 GHz were raised in the Rx direction and measured as shown in Table 3.7.

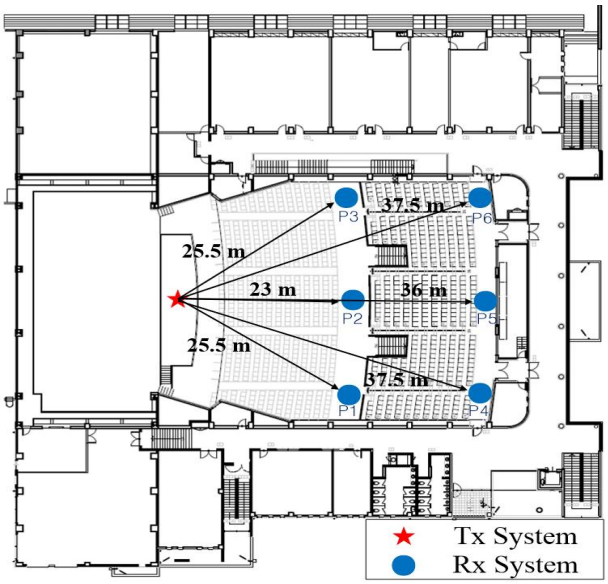

Figure 3.7. Floor plan of a large auditorium

Table 3.7. Key parameters for measurement in scenario (6)

Frequency [GHz]	Antenna	SG Power [dB]	Cable Loss [dB]	Antenna Gain [dB]	Power [dB]
3.7	Horn	0	2.8	10	7.2
	ODA				
28	Horn	0	9.4	20	10.6
	TAS				

조선대학교
CHOSUN UNIVERSITY

7. Scenario (7) : Open Ten-story Staircase

In the seventh scenario, measurements were performed on the internal staircase of Chosun University's IT Convergence University as shown in Figure 3.8. The height of the stair is 17 cm. The skip floor has a length, width, and height of 6.7 m, 3.4 m, and 3.8 m, respectively. It consists of 12 stairs. After Tx was installed on the first floor and the doors and windows of all the staircase were closed, Rx was measured at nine points, one floor from the second floor (see Table 3.8). The reception strength was weak after the fourth floor in the 3.7 GHz band. Therefore, the transmission power from the 5th to the 10th floor was increased by 20 dB. It was not measured in the 28 GHz band because of the low reception intensity.

Figure 3.8. Open ten-story staircase

Table 3.8. Key parameters for measurement in scenario (7)

Frequency [GHz]	Antenna	SG Power [dB]	Cable Loss [dB]	Antenna Gain [dB]	Power [dB]
3.7	Horn	0 / 20	2.8	10	7.2 / 27.2
	ODA	0 / 20	2.8	10	7.2 / 27.2

조선대학교
CHOSUN UNIVERSITY

8. Scenario (8) : Closed Six-story Staircase

In the eighth scenario, measurements were performed in the closed staircase environment of the Chosun University Industry-Academic Cooperation Foundation. It is a building with six floors. Unlike general staircase, the stairs going up and down are blocked by walls as shown in Figure 3.9. It is a space with a length, width and height of 8 m, 2.5 m, and 3.6 m, respectively. The height of the stair is 13 cm for the skip floor and 15 cm for the main floor. Tx was installed in the upward direction of the first floor. Rx was measured in a closed environment from the stairs in front of the entrance of each floor at a total of five points, sequentially from the second floor.

Figure 3.9. Closed six-story staircase

Table 3.9. Key parameters for measurement in scenario (8)

Frequency [GHz]	Antenna	SG Power [dB]	Cable Loss [dB]	Antenna Gain [dB]	Power [dB]
3.7	Horn	20	2.8	10	27.2
	ODA				
28	Horn	20	9.4	20	30.6

조선대학교
CHOSUN UNIVERSITY

Ⅳ. Measurement and Analysis of Propagation Path Loss

A. Measurement and Analysis of Propagation Path Loss in Indoor Building Corridor Environment

Figure 4.1 illustrates the results of analyzing the measured and predicted values of propagation path loss in the 3.7 GHz and 28 GHz bands in the normal corridor, which is the LOS environment in scenario (1).

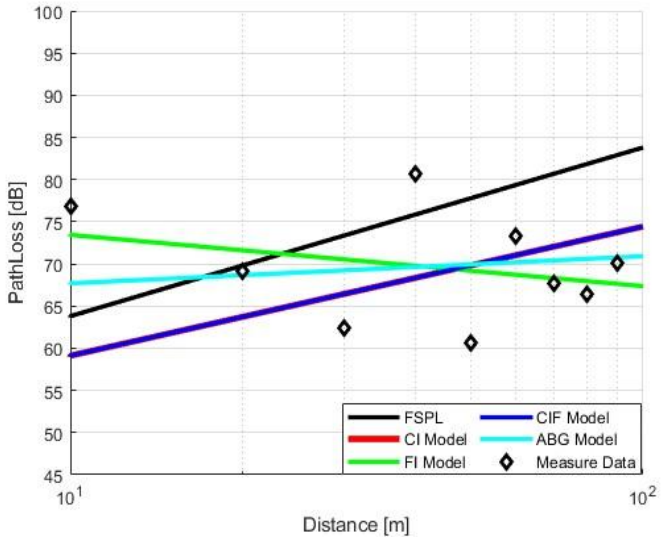

(a) 3.7 GHz Horn Ant.

조선대학교
CHOSUN UNIVERSITY

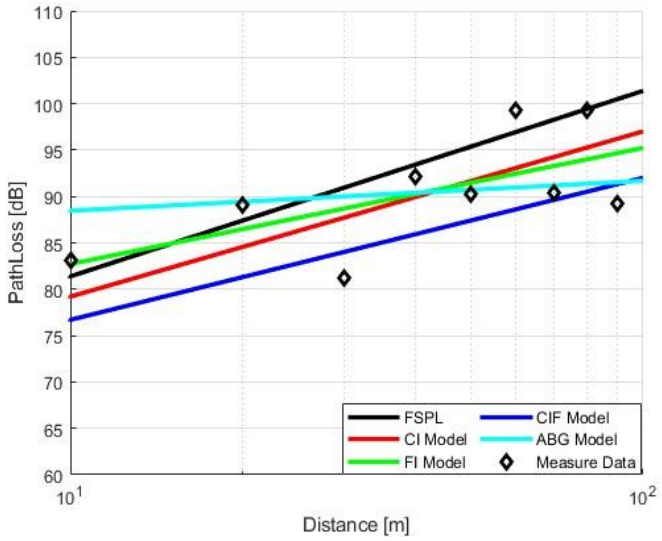

(b) 28 GHz Horn Ant.

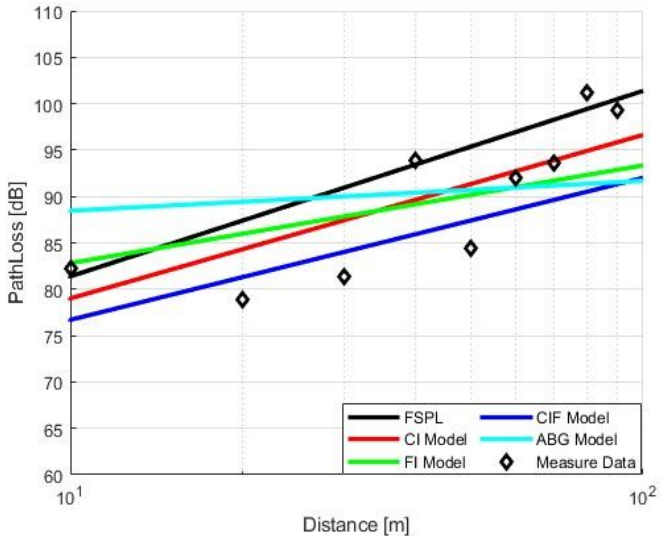

(c) 28 GHz TAS

Figure 4.1. Measured and predicted values in scenario (1)

According to Figure 4.1, the standard was approximately 6.4 in the ABG model in a directional horn antenna at 3.7 GHz. This was similar to most actual measurement data. However, each of CI and CIF models had a value of approximately 8.6 and was the

조선대학교
CHOSUN UNIVERSITY

least suitable. The 28 GHz directional horn antenna had a standard deviation of approximately 4.5 in the FI model and was similar to the measurement data. However, it had a value of approximately 8.6 in the CI model and is the least suitable. The measurement at 28 GHz using a TAS capable of receiving radio waves in all directions showed the lowest path loss at the rear of the TAS owing to reflection and diffraction of the glass doors at the end of the corridor. This was unlike the directional horn antenna. The standard deviation in the FI model was approximately 4.6. The ABG model was the least suitable at approximately 7.0.

Table 4.1. Parameters of the propagation path loss model derived from scenario (1)

Freq. (GHz)	Ant.	CI (n)	FI (α)	FI (β)	CIF (n)	CIF (b)	ABG (α)	ABG (β)	ABG (γ)
3.7	Horn	1.53	79.53	-0.61	1.69	0.12	0.32	51.06	2.36
28	Horn	1.78	70.20	1.25					
	TAS	1.76	55.58	2.11					

Table 4.1 shows the coefficients of radio path loss models derived when measured by directional horn antennas and TAS in the 3.7 GHz and 28 GHz bands in the normal corridor of scenario (1).

The results of Table 4.1 show that the PLE of the CI model with an independent coefficient was most similar to the free space when measured by a directional horn antenna in the 28 GHz band.

Figure 4.2 shows the results of an analysis of the measured and predicted values of propagation path loss in the 3.7 GHz and 28 GHz bands in the long corridor, which is the LOS environment in scenario (2).

조선대학교
CHOSUN UNIVERSITY

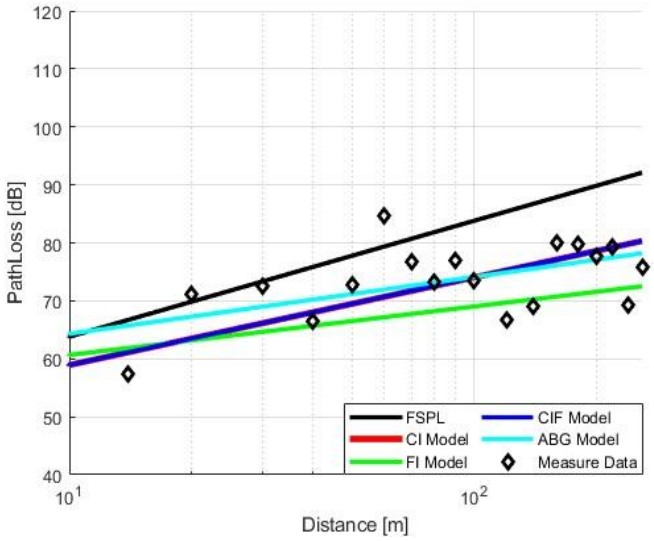

(a) 3.7 GHz Horn Ant.

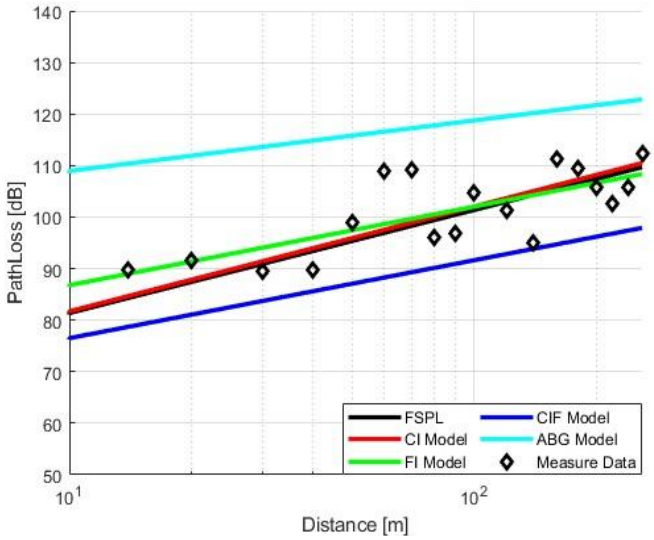

(b) 28 GHz Horn Ant.

Figure 4.2. Measured and predicted values in scenario (2)

According to Figure 4.2, the standard deviation of the FI model at 3.7 GHz was approximately 5.3. This was similar to most actual measurement data. The graphs and standard deviation were similar to the remaining models. Even at 28 GHz, it had a

조선대학교
CHOSUN UNIVERSITY

standard deviation of approximately 5.2 in the FI model and showed the highest similarity. It had a value of approximately 7.4 in the ABG model and was the least suitable.

Table 4.2. Parameters of the propagation path loss model derived from scenario (2)

Freq. (GHz)	Ant.	CI. (n)	FI (α)	FI (β)	CIF (n)	CIF (b)	ABG (α)	ABG (β)	ABG (γ)
3.7	Horn	1.51	57.27	0.84	1.77	0.19	0.98	25.67	5.08
28	Horn	2.03	71.54	1.52					

Table 4.2 shows the coefficients of each path loss prediction model derived when measured with a directional horn antenna in the 3.7 GHz and 28 GHz bands in the main building of approximately 375 m of scenario (2).

Table 4.2 reveals that the PLE in the 28 GHz band was more similar to the free space than that in the 3.7 GHz band. Figure 4.3 shows the results of an analysis of the measured and predicted values of propagation path loss in the 3.7 GHz and 28 GHz bands in a circular building, which is an NLOS environment in scenario (3). Since the environment is fixed so that the directions of Tx and Rx face each other, the prediction is inaccurate as the characteristics of propagation by diffraction, reflection, scattering, etc. are applied by the curved wall.

조선대학교
CHOSUN UNIVERSITY

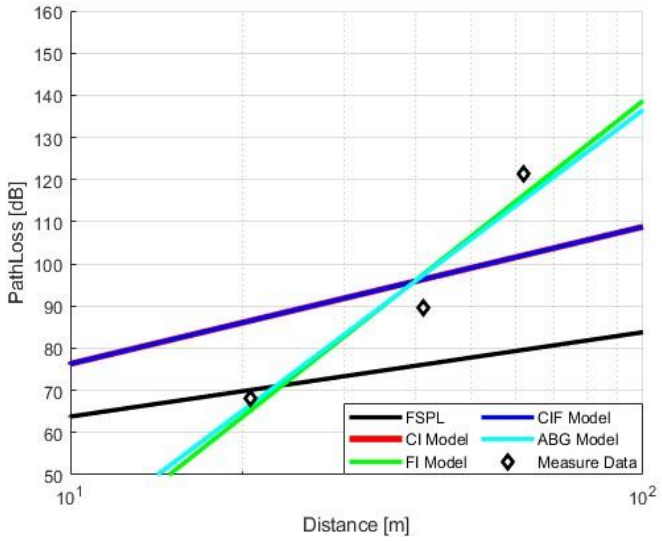

(a) 3.7 GHz Horn Ant.

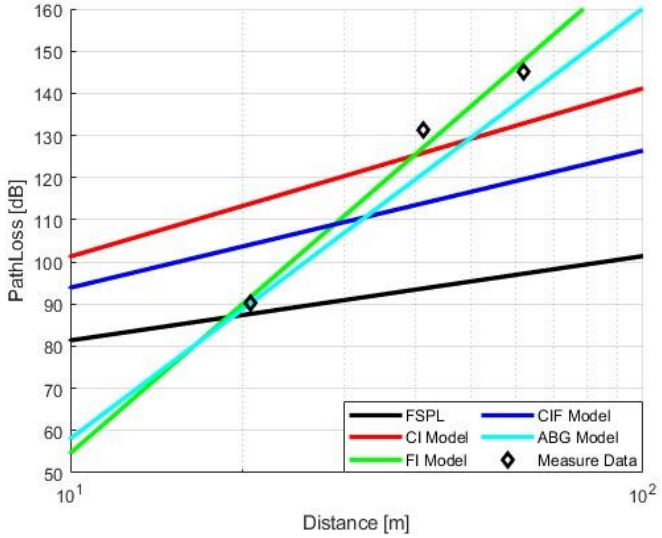

(b) 28 GHz Horn Ant.

조선대학교
CHOSUN UNIVERSITY

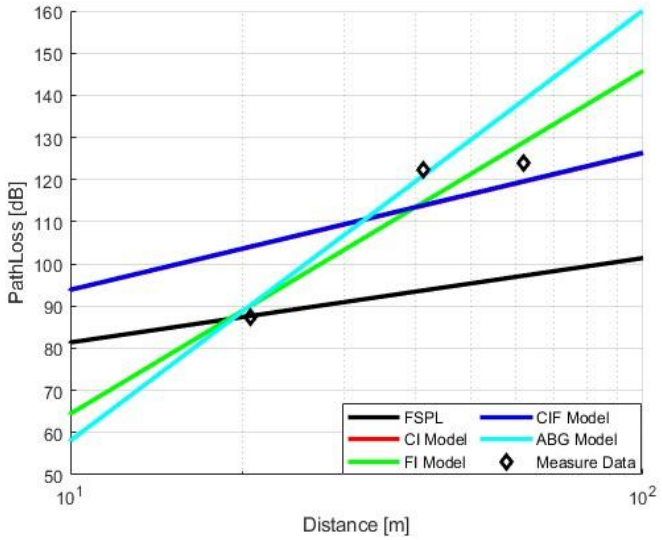

(c) 28 GHz TAS

Figure 4.3. Measured and predicted values in scenario (3)

According to Figure 4.3, the FI model was the most similar at 3.7 GHz, with a standard deviation of approximately 5.6. However, the CI and CIF models were not the most suitable and have a standard deviation of approximately 15.8. The FI model was most similar at 28 GHz, had a standard deviation of approximately 3.0, and was the least suitable for CI and CIF models. The overall path loss was reduced when the measurement was performed through the TAS. The FI model was the most suitable and had a standard deviation of approximately 5.5. However, it had a standard deviation of approximately 16.3 in the CIF model and was the least suitable.

Table 4.3. Parameters of the propagation path loss model derived in scenario (3)

Freq. (GHz)	Ant.	CI (n)	FI (α)	FI (β)	CIF (n)	CIF (b)	ABG (α)	ABG (β)	ABG (γ)
3.7	Horn	3.25	-75.65	10.72	3.49	0.09	10.20	-82.84	2.69
28	Horn	3.99	-62.98	11.76					
	TAS	3.24	-16.90	8.13					

조선대학교
CHOSUN UNIVERSITY

Table 4.3 shows the coefficients of the propagation path loss prediction models derived from the directional horn antenna and TAS in a circular building with an indoor circumference of approximately 82.7 m in scenario (3).

According to Table 4.3, the PLE of the CI model with a single coefficient was significantly low compared with the free space. The measurement method using TAS in the NLOS environment was relatively good.

B. Measurement and Analysis of Propagation Path Loss in Tunnel Environment

Figure 4.4 shows the results of analyzing the measured and predicted values of propagation path loss in the 3.7 GHz and 28 GHz bands in the LOS environment in scenario (4).

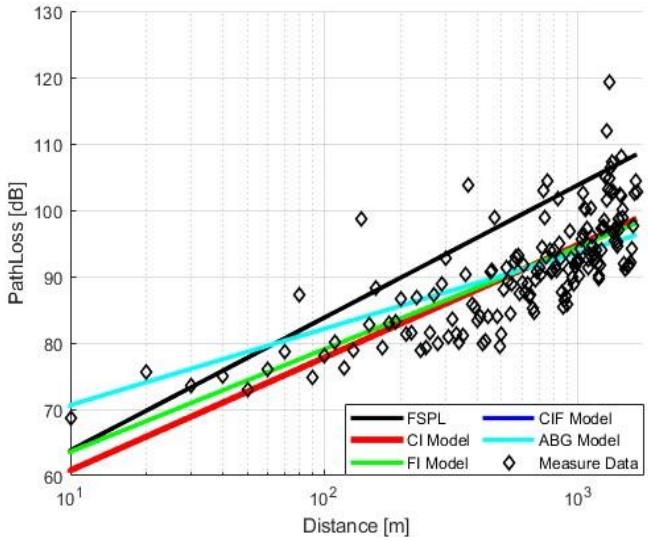

(a) 3.7 GHz Horn Ant.

조선대학교
CHOSUN UNIVERSITY

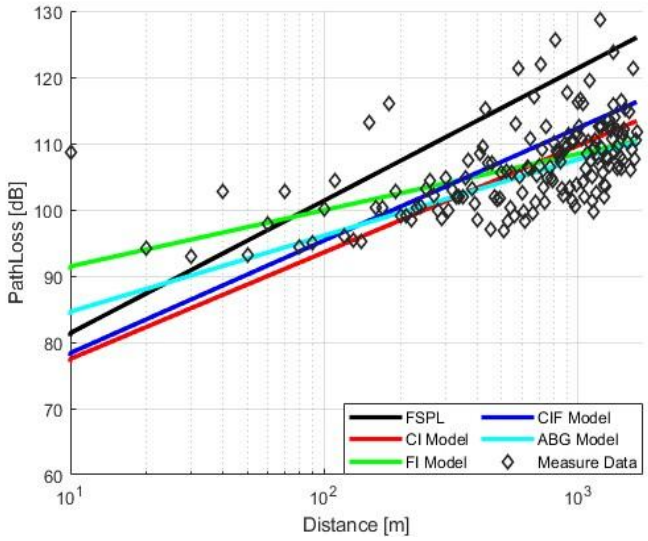

(b) 28 GHz Horn Ant.

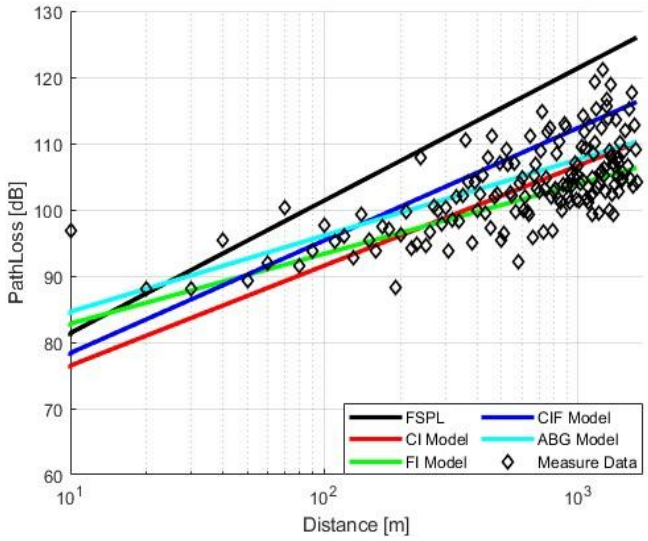

(c) 28 GHz TAS

Figure 4.4. Measured and predicted values in scenario (4)

Figure 4.4 shows that the FI model was the most suitable for the 3.7 GHz and 28 GHz band of directional horn antennas, with a standard deviation of approximately 5.5.

조선대학교
CHOSUN UNIVERSITY

However, the ABG model was not the most suitable in the 3.7 GHz band and had a standard deviation of approximately 5.7. The CI model had a standard deviation of approximately 6.4 in the 28 GHz band. The method using TAS showed similarities with an average standard deviation of approximately 5.0 in all the models.

Table 4.4. Parameters of the propagation path loss model derived from scenario (4)

Freq. (GHz)	Ant.	CI (n)	FI (α)	FI (β)	CIF (n)	CIF (b)	ABG (α)	ABG (β)	ABG (γ)
3.7	Horn	1.70	48.15	1.54	1.61	-0.07	1.15	50.10	1.59
28	Horn	1.61	82.97	0.85					
	TAS	1.5	74.27	1.05					

Table 4.4 shows the coefficients of the propagation path loss prediction models derived when measured with directional horn antennas and TAS in the 3.7 GHz and 28 GHz bands in a tunnel of approximately 1,700 m in scenario (4).

Table 4.4 shows that the PLE of the CI model in the 3.7 GHz band was similar to the free space compared with that for the 28 GHz band, owing to the characteristics of the frequency.

C. Measurement and Analysis of Propagation Path Loss in Indoor Auditorium Environment

Figure 4.5 shows the analysis results of propagation path loss measurements and predicted values in the 3.7 GHz and 28 GHz bands in the small auditorium, which is the LOS environment in scenario (5).

조선대학교
CHOSUN UNIVERSITY

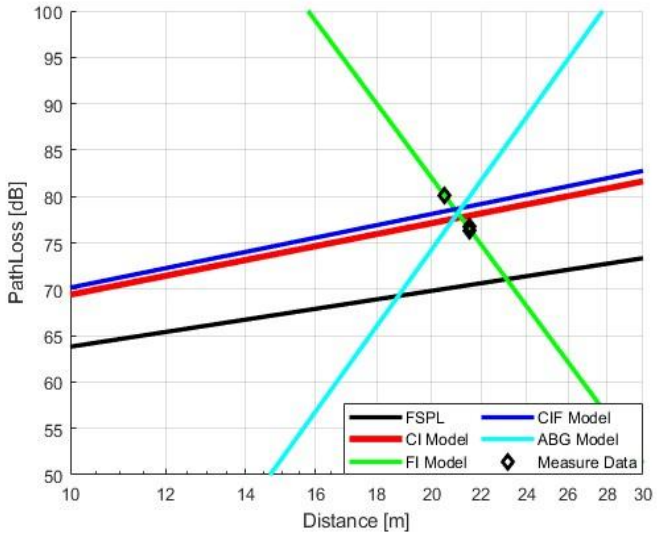

(a) 3.7 GHz Horn Ant.

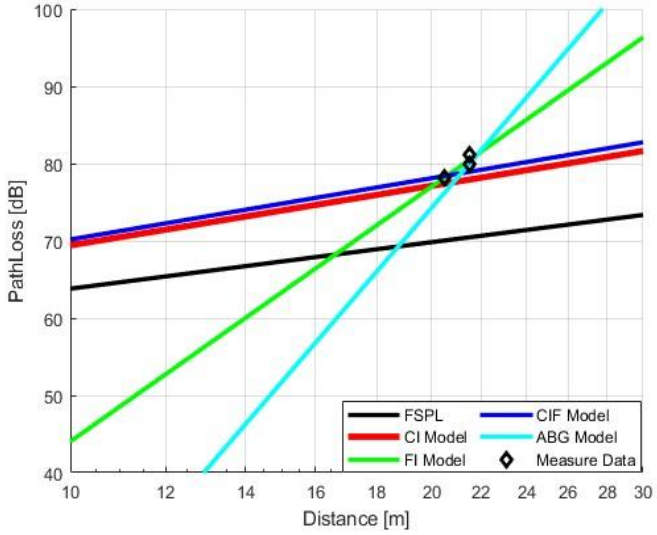

(b) 3.7 GHz ODA

조선대학교
CHOSUN UNIVERSITY

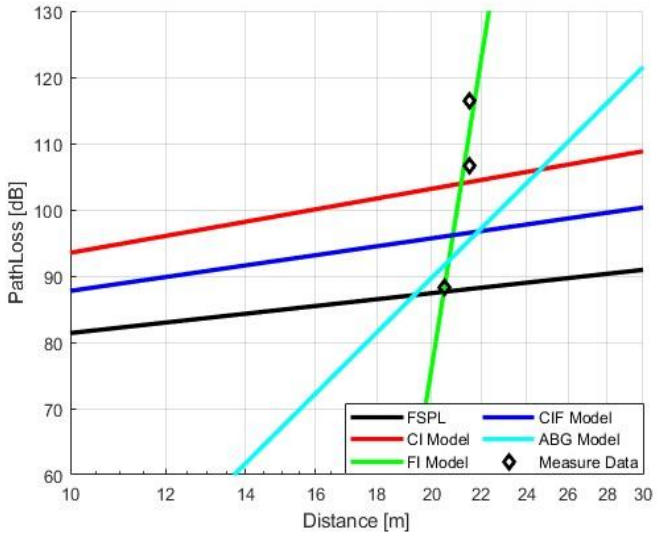

(c) 28 GHz Horn Ant.

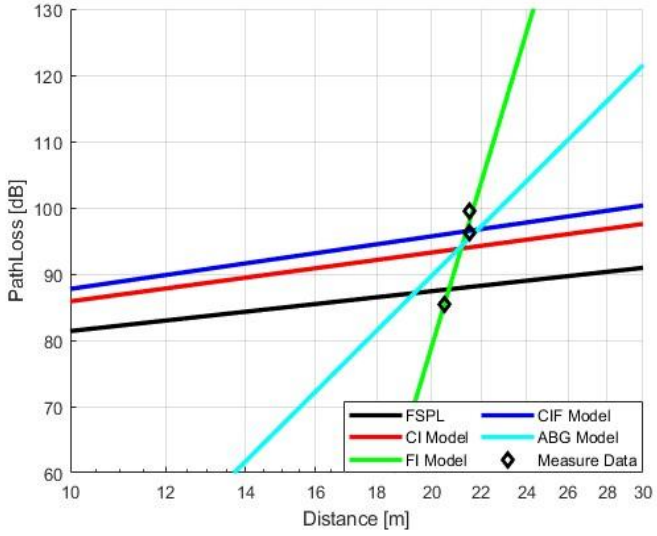

(d) 28 GHz TAS

Figure 4.5. Measured and predicted values in scenario (5)

It is evident from Figure 4.5 that the FI model had a significantly small standard deviation of approximately 0.2 in the directional horn antenna in the 3.7 GHz band. It was unsuitable and had a standard deviation of approximately 2.2 in the CIF model. In

조선대학교
CHOSUN UNIVERSITY

the ODA in the 3.7 GHz band, all the models had a standard deviation of less than one. This revealed similarities. The directional horn antennas in the 28 GHz band were the most similar with a standard deviation of approximately 4.0 in the FI model. It was unsuitable in the CI and CIF models, and had standard deviations of 11.4 and 12.5, respectively. In the TAS, the FI model also had a standard deviation of approximately 1.3, and the CI and CIF models had standard deviations of approximately 5.8 and 7.7, respectively. This showed that it was the most unsuitable.

Table 4.5. Parameters of the propagation path loss model derived from scenario (5)

Freq. (GHz)	Ant.	CI (n)	FI (α)	FI (β)	CIF (n)	CIF (b)	ABG (α)	ABG (β)	ABG (γ)
3.7	Horn	2.56	309.44	-17.48	2.73	0.05	18.06	-170.64	1.76
	ODA	2.71	-65.59	10.96					
28	Horn	3.21	-1390.05	112.70					
	TAS	2.45	-702.48	60.07					

Table 4.5 shows the coefficients of radio path loss prediction models derived from directional horn antennas and ODA in the 3.7 GHz band in the small auditorium of scenario (5), and directional horn antennas and TAS at 28 GHz.

The results of Table 4.5 show that PLE was the most similar to the free space in a directional horn antenna in the 3.7 GHz band and the least similar in a directional horn antenna in the 28 GHz band.

As shown in scenario (6), the angle of Tx was measured by increasing the angle of Tx by 15° in the Rx direction in a 3.7 GHz and 28 GHz directional horn antenna in a large auditorium of Chosun University, and by using a 3.7 GHz ODA and 28 GHz TAS.

조선대학교
CHOSUN UNIVERSITY

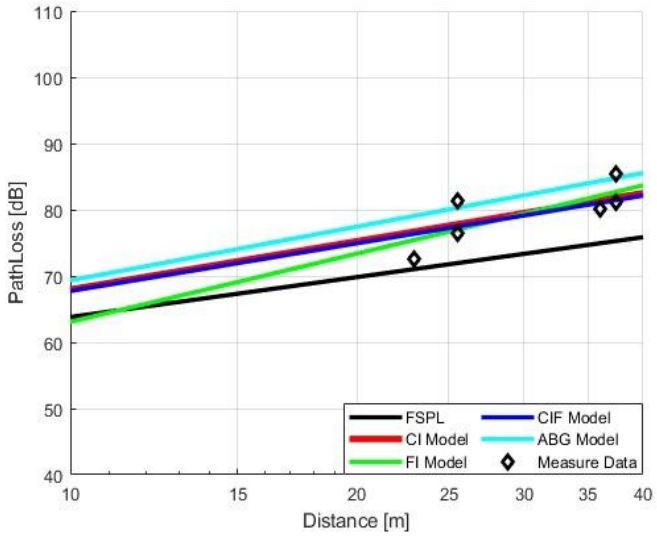

(a) 3.7 GHz Horn Ant.

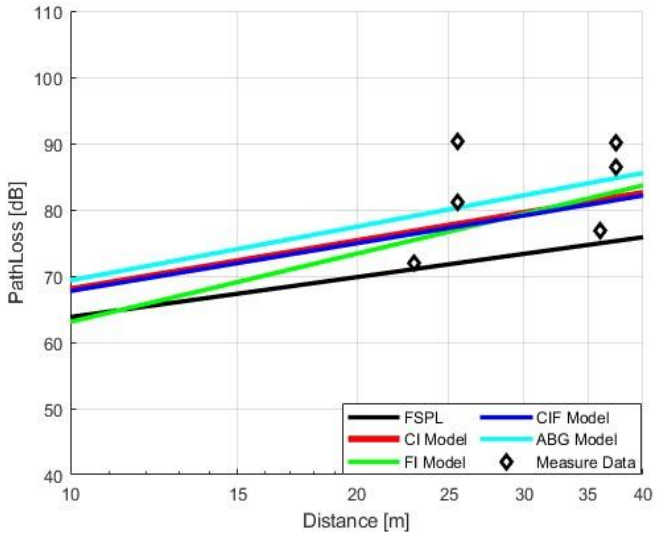

(b) 3.7 GHz Horn Ant. (15 tilt)

조선대학교
CHOSUN UNIVERSITY

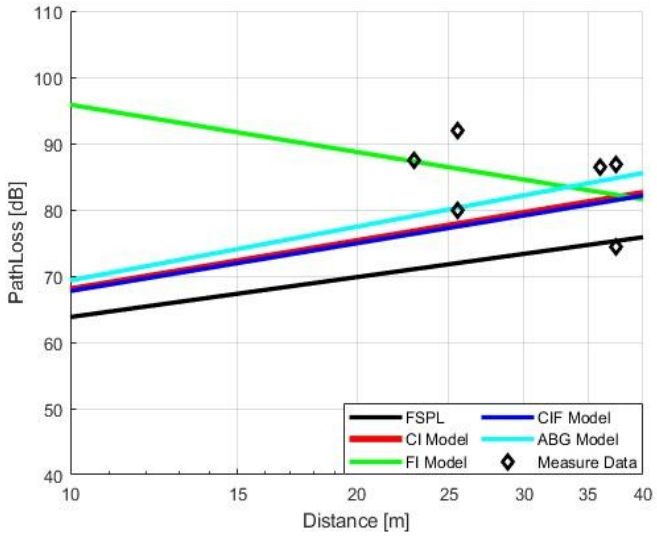

(c) 3.7 GHz ODA

Figure 4.6. Measured and predicted values for 3.7 GHz band in scenario (6)

In a 3.7 GHz directional horn antenna, all the models had a standard deviation of approximately 2.5 and were similar to the measurement data. As illustrated in Figure 4.6, the path loss increased when the antenna angle of Tx was increased by 15°. The ABG model was the most suitable with a standard deviation of approximately 4.1. In the ODA at 3.7 GHz, the ABG model was the most suitable with a standard deviation of approximately 4.8 and the FI model was the most unsuitable with a standard deviation of approximately 8.7.

Table 4.6. Parameters of the propagation path loss model derived in the 3.7 GHz band of scenario (6)

Freq. (GHz)	Ant.	CI (n)	FI (α)	FI (β)	CIF (n)	CIF (b)	ABG (α)	ABG (β)	ABG (γ)
3.7	Horn	2.42	28.85	3.42	2.74	0.16	2.69	26.436	2.81
	Horn (15° tilt)	2.64	39.18	2.95					
	ODA	2.73	119.52	-2.37					

조선대학교
CHOSUN UNIVERSITY

Table 4.6 shows the coefficients of each model when measured by raising the directional horn antenna of 3.7 GHz and that of Tx in the basic angle and 15° Rx direction in a large auditorium in scenario (6).

As shown in Table 4.6, the PLE of the CI model in the 3.7 GHz band was similar to each other.

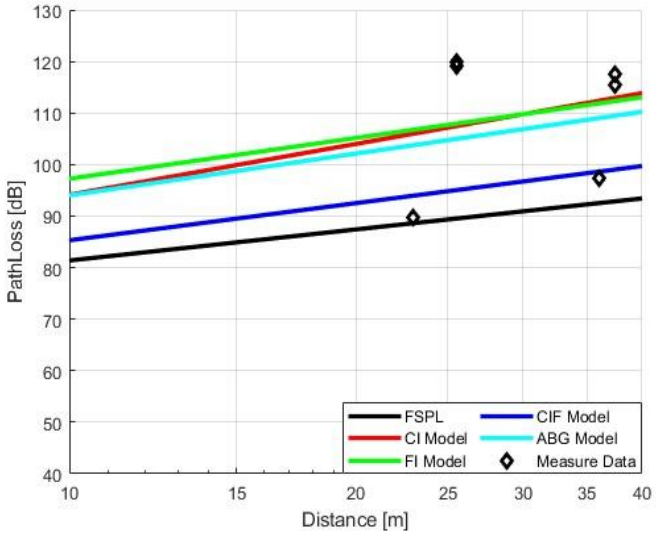

(a) 28 GHz Horn Ant.

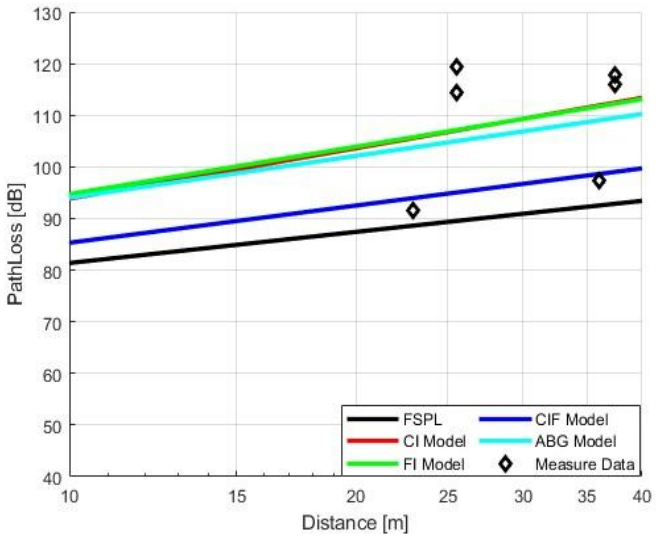

(b) 28 GHz Horn Ant. (15 tilt)

조선대학교
CHOSUN UNIVERSITY

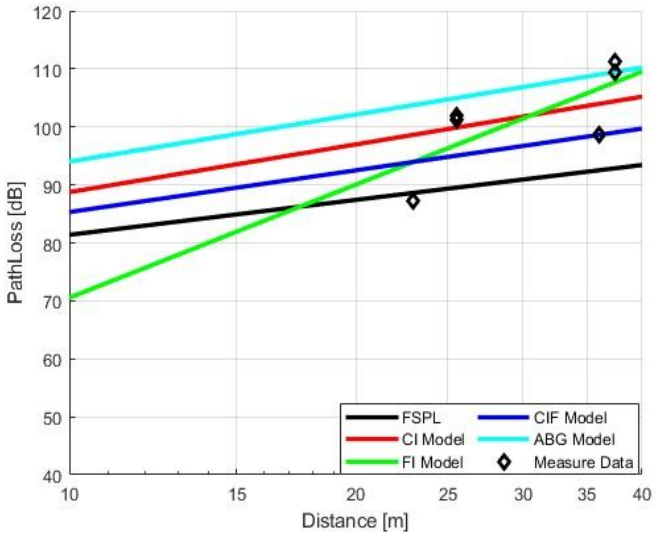

(c) 28 GHz TAS

Figure 4.7. Measured and predicted values for the 28 GHz band in scenario (6)

Figure 4.7 shows that in a directional horn antenna at 28 GHz, the ABG model had a standard deviation of approximately 8.3. The remaining models had a standard deviation of approximately 12.0. No significant difference in path loss occurred because the measurement was performed by raising the antenna of Tx by 15°. The ABG model had a standard deviation of approximately 7.1, and the remaining models had a standard deviation of approximately 10.5. The measurement method by TAS showed that 1) the path loss was reduced significantly compared with the directional horn antenna, 2) the FI model had a standard deviation of approximately 5.3, 3) the CIF model had a standard deviation of approximately 8.1 and was the most unsuitable.

조선대학교
CHOSUN UNIVERSITY

Table 4.7. Parameters of the propagation path loss model derived in the 28 GHz band of scenario (6)

Freq. (GHz)	Ant.	CI (n)	FI (α)	FI (β)	CIF (n)	CIF (b)	ABG (α)	ABG (β)	ABG (γ)
28	Horn	3.28	71.00	2.63	2.74	0.16	2.69	26.44	2.81
	Horn (15° tilt)	3.24	64.18	3.05					
	TAS	2.74	5.74	6.48					

Table 4.7 shows the coefficients of propagation path loss prediction models derived when measured in a manner similar to that in Table 4.6 in the 28 GHz band in the large-sized auditorium environment of scenario (6).

The results of Table 4.7 show that unlike Table 4.6, the PLE in the 3.7 GHz band is dissimilar to the free space. Furthermore, the PLE values in TAS are similar in the 3.7 GHz and 28 GHz bands.

D. Measurement and Analysis of Propagation Path Loss in Staircase Environment

It was measured using a 3.7 GHz directional horn antenna and an ODA for each floor in an open general staircase, which is an NLOS environment in scenario (7). The reception strength was non-uniform after the fourth layer. The antenna strength of Tx was increased by 20 dB to measure it. However, the propagation path loss in the 28 GHz band was highly severe and could not be measured.

조선대학교
CHOSUN UNIVERSITY

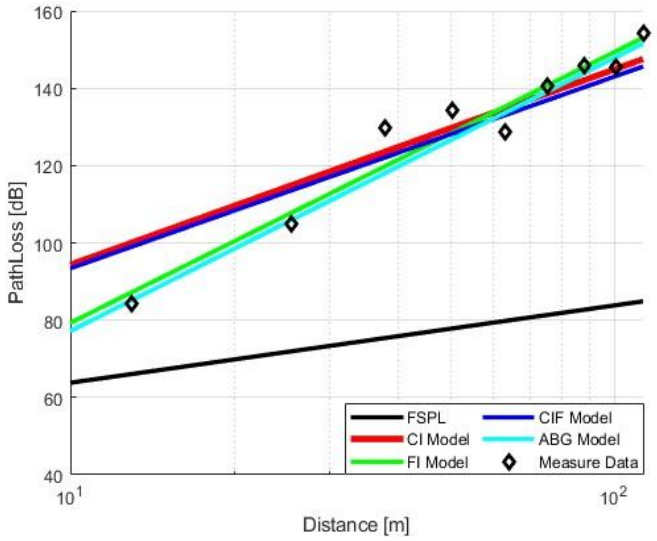

(a) 3.7 GHz Horn Ant.

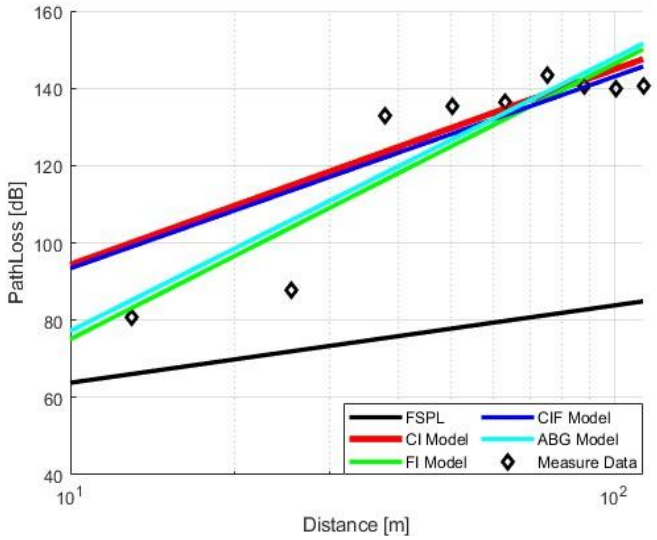

(b) 3.7 GHz ODA

Figure 4.8. Measured and predicted values in scenario (7)

From Figure 4.8, the FI and ABG models were most suitable for directional horn antennas and ODA at 3.7 GHz. The standard deviations for the directional horn antenna were 4.8 and 5.1, respectively, which were most suitable. In an ODA, the path loss

조선대학교
CHOSUN UNIVERSITY

was lower than that of a directional horn antenna, and the standard deviations were approximately 9.7 and 9.8 (two times as high).

Table 4.8. Parameters of the propagation path loss model derived from scenario (7)

Freq. (GHz)	Ant.	CI (n)	FI (α)	FI (β)	CIF (n)	CIF (b)	ABG (α)	ABG (β)	ABG (γ)
3.7	Horn	5.05	9.25	7.00	4.96	2.15	7.06	-115.61	21.50
	ODA	4.87	3.90	7.12					

Table 4.8 shows the coefficients of propagation path loss prediction models derived when measured with directional horn antennas and ODA in the 3.7 GHz band of the open ten-story stairs of scenario (7).

From Table 4.8, the PLE value was significantly low.

Similar to scenario (8), the propagation path was measured by raising the signal generator on the Tx side by 20 dB using a 3.7 GHz directional horn antenna, an ODA, and a 28 GHz directional horn antenna on each floor in a closed staircase of a six-story circular building. The results of loss measurement and predicted value analysis are shown in Figure 4.9.

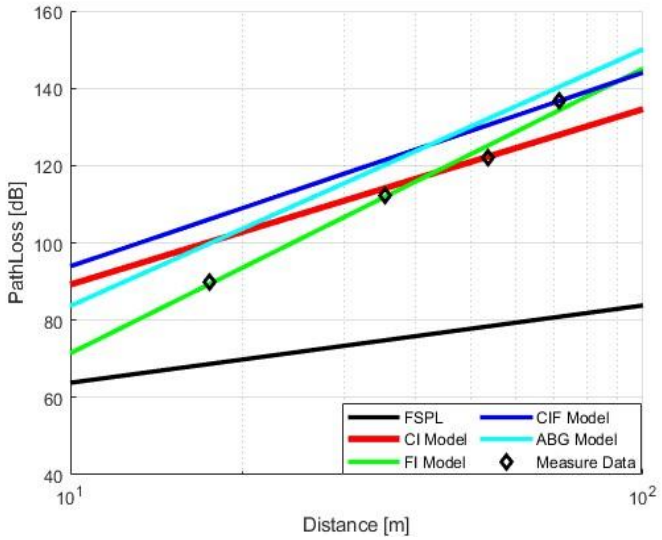

(a) 3.7 GHz Horn Ant.

조선대학교
CHOSUN UNIVERSITY

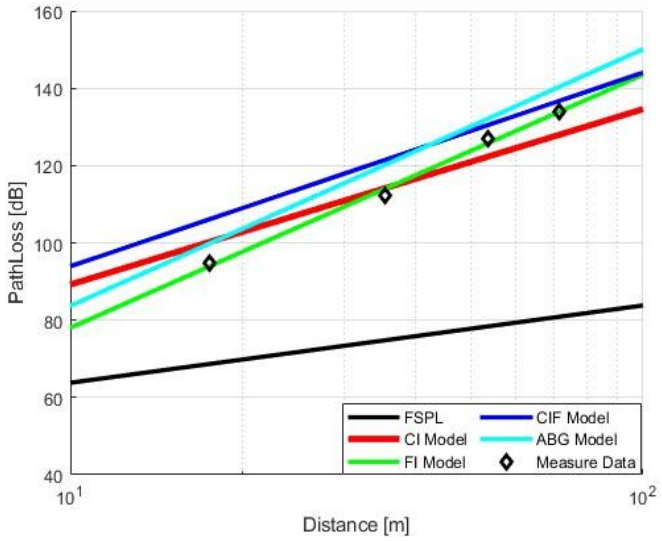

(b) 3.7 GHz ODA

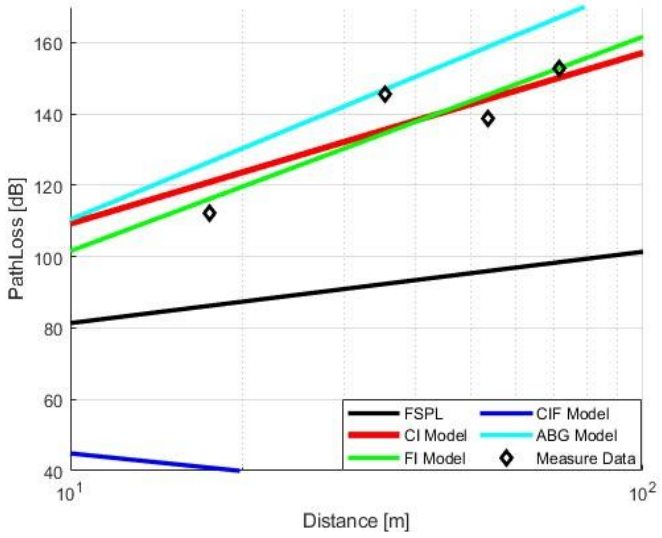

(c) 28 GHz Horn Ant.

Figure 4.9. Measured and predicted values in scenario (8)

The results in Figure 4.9 show that the standard deviation of the ABG model in a 3.7 GHz directional horn antenna was approximately 5.6, which was the most suitable. The standard deviation of approximately 10.2 in the CIF model was the least suitable.

조선대학교
CHOSUN UNIVERSITY

Although the difference in path loss was marginal in the ODA, the standard deviation in the FI model was the most suitable at approximately 1.1. The standard deviation in the CIF model was approximately 7.7, which displayed the least suitability. For directional horn antennas at 28 GHz, the FI model is most suitable with a standard deviation of 6.6. The CIF had a standard deviation of approximately 121.2 and was unsuitable.

Table 4.9. Parameters of the propagation path loss model derived from scenario (8)

Freq. (GHz)	Ant.	CI (n)	FI (α)	FI (β)	CIF (n)	CIF (b)	ABG (α)	ABG (β)	ABG (γ)
3.7	Horn	4.54	-2.24	7.37	2.79	-1.16	6.64	0.0001	3.04
	ODA	4.63	12.54	6.55					
28	Horn	4.79	41.53	6.01					

Table 4.9 shows the coefficients of propagation path loss prediction models derived from the 3.7 GHz band of the closed six-story staircase of scenario (8), measured from the directional horn antenna and from the 28 GHz band.

Table 4.9 shows that the value of PLE was relatively better than that presented in Table 4.8.

조선대학교
CHOSUN UNIVERSITY

E. Comparison of Propagation Path Loss Model

Table 5.1. Fit model by scenario

Location	Frequency	Antenna	Fit Model	Unfit Model
Normal Corridor	3.7 GHz	Horn	ABG	CI, CIF
	28 GHz	Horn	FI	CI
		TAS	FI	ABG
Long Corridor	3.7 GHz	Horn	FI	-
	28 GHz	Horn	FI	ABG
Circular Corridor	3.7 GHz	Horn	FI	CI, CIF
	28 GHz	Horn	FI	CI, CIF
		TAS	FI	CIF
Tunnel	3.7 GHz	Horn	FI	ABG
	28 GHz	Horn	FI	CI
		TAS	ALL	-
Small Auditorium	3.7 GHz	Horn	FI	CIF
		ODA	ALL	-
	28 GHz	Horn	FI	CI, CIF
		TAS	FI	CI, CIF
Large Auditorium	3.7 GHz	Horn	ALL	-
		Horn	ABG	-
		ODA	ABG	FI
	28 GHz	Horn	ABG	-
		Horn	ABG	-
		TAS	FI	CIF
Open Staircase	3.7 GHz	Horn	FI, ABG	-
		ODA	FI, ABG	-
Closed Staircase	3.7 GHz	Horn	ABG	CIF
		ODA	FI	CIF
	28 GHz	Horn	FI	CIF

조선대학교
CHOSUN UNIVERSITY

The results of a comparison of the propagation path loss model based on the results of Figures 4.1～4.9 and Tables 4.1～4.9 are shown in Table 5.1.

According to Table 5.1, when measured with a directional horn antenna in the 3.7 GHz band, five scenarios were suitable for the FI model, and four were suitable for the ABG model. There is one scenario in which a model that was all suitable. However, the unsuitable model showed that two scenarios in the CI model, four in the CIF model, and one in the ABG model were unsuitable. When measured with an ODA, two scenarios were suitable for the FI model, and two were suitable for the ABG model. All the models were suitable in one scenario. However, the unsuitable model showed that a scenario in the FI model and one in the CIF model were unsuitable.

In a directional horn antenna in the 28 GHz band, six scenarios for the FI model and two for the ABG model were suitable. It was shown that four scenarios for the CI model, three for the CIF model, and one for the ABG model were unsuitable. In the measurement by TAS, four scenarios for the FI model and one for all the models were suitable. One scenario for the CI model, three for the CIF model, and one for the ABG model were unsuitable.

조선대학교
CHOSUN UNIVERSITY

Ⅴ. Conclusion

Actual measured results for various environments in the 3.7 GHz and 28 GHz bands used in 5G communication systems were compared and analyzed through propagation path loss models (CI, FI, CIF, and ABG).

I showed that it is reasonable to use a 1 m reference distance FSPL even in NLOS environments. This is because the propagation signal does not hit the obstruction or structure of the first propagation even when Rx is located in the NLOS environment.

When each scenario was compared based on the PLE value of the CI model with a single parameter among the path loss prediction models, it was most similar to the PLE of free space in the 28 GHz band of the indoor building environment. The tunnel was similar in the 3.7 GHz band. In the small auditorium, the TAS in the 28 GHz band was most similar to the PLE. In the large auditorium, the PLE of the directional horn antenna was most similar to the free space in the 3.7 GHz band. It was shown that the PLE values of the ODA at 3.7 GHz and the TAS at 28 GHz were highly similar. The PLE value in the stair environment was significantly low compared with other scenarios. The closed type was better than the open type.

In the entire scenario, the FI model was shown to be the most suitable, and the CIF model was shown to be the least suitable. The FI model and ABG model were the most suitable in the 3.7 GHz band, and the CIF model was unsuitable. In the 28 GHz band, the FI model was the most suitable, and the CIF and CI models were the least suitable. When the path loss model was compared in a specific environments, the actual measured value and predicted value of the FI model were the most similar.

The results of this study would help develop an efficient and stable mmWave indoor small cell network.

조선대학교
CHOSUN UNIVERSITY

References

[1] A. M. Al-Samman, T. A. Rahman, M. H. Azmi, M. N. Hindia, I. Khan, and E. Hanafi, "Statistical Modelling and Characterization of Experimental mm-Wave Indoor Channelsfor Future 5G Wireless Communication Networks," PloS one, Vol. 11, No. 9, Sep. 2016.

[2] Ahmed Mohammed Al-Samman, Tharek Abd. Rahman, Tawfik Al-Hadhrami, Abdusalama Daho, MHD Nour Hindia, Marwan Hadri Azmi, Kaharudin Dimyati, and Mamoun Alazab, "Comparative Study of Indoor Propagation Model Below and Above 6 GHz for 5G Wireless Networks," Electronics, Vol. 8, No. 1, Jan. 2019.

[3] Dmitry Chizhik, Jinfeng Du, Rodolfo Feick, Mauricio Rodriguez, Guillermo Castro, and Reinaldo A. Valenzuela, "Path Loss and Directional Gain Measurements at 28 GHz for Non-Line-of-Sight Coverage of Indoors With Corridors," IEEE Transactions on Antennas and Propagation, Vol. 68, No. 6, pp. 4820-4830, Jun. 2020.

[4] Shuai Nie, George R. MacCartney Jr., Shu Sun, and Theodore S. Rappaport, "72 GHz Millimeter Wave Indoor Measurements for Wireless and Backhaul Communications," 2013 IEEE 24th Annual International Symposium on Personal, Indoor, and Mobile Radio Communications (PIMRC), pp. 2429-2433, Nov. 2013.

[5] George R. Maccartney, Theodore S. Rappaport, Shu Sun, and Sigia Deng, "Indoor Office Wideband Millimeter-Wave Propagation Measurements and Channel Models at 28 and 73 GHz for Ultra-Dense 5G Wireless Networks," IEEE Access, Vol. 3, pp. 2388-2424, Oct. 2015.

[6] Ahmed M. Al-Samman, Marwan Hadri Azmi, Y. A. Al-Gumaei, Tawfik Al-Hadhrami, Tharek Abd. Rahman, Yousef Fazea, and Abdulmajid Al-Mqdashi, "Millimeter Wave Propagation Measurements and Characteristics for 5G System," Applied Sciences, Vol. 10, No. 1, Jan. 2020.

[7] Hasan F. Ates, Syed Muhammad Hashir, Tuncer Baykas, and Bahadir K. Gunturk, "Path Loss Exponent and Shadowing Factor Prediction From Satellite Images Using Deep Learning," IEEE Access, Vol. 7, pp. 101366-101375, Jul. 2019.

[8] Nicholas O. Oyie, and Thomas J. O. Afullo, "Measurements and Analysis of

조선대학교
CHOSUN UNIVERSITY

Large-Scale Path Loss Model at 14 and 22 GHz in Indoor Corridor," IEEE Access, Vol. 6, pp. 17205-17214, Feb. 2018.

[9] Mohammed Bahjat Majed, Tharek Abd Rahman, Omar Abdul Aziz, Mohammad Nour Hindia, and Effariza Hanafi, "Channel Characterization and Path Loss Modeling in Indoor Environment at 4.5, 28, and 38GHz for 5G Cellular Networks," International Journal of Antennas and Propagation, Vol. 2018, Sep. 2018.

[10] Feyisa Debo Diba, Md Abdus Samad, and Dong-You Choi, "Centimeter and Millimeter-Wave Propagation Characteristics for Indoor Corridors: Results rom Measurements and Models," IEEE Access, Vol. 9, pp. 158726-158737, Nov. 2021.

[11] Ju-yul Lee, Jinyi Liang, Myung-Don Kim, Jae-Joon Park, Bong-hyuk Park and Hyun-Kyu Chung, "Measurement-Based Propagation Channel Characteristics for Millimeter-Wave 5G Giga Communication Systems," ETRI Journal, Vol. 38, No. 6, pp. 1031-1041, Dec. 2016.

[12] Yuyan Shen, Yu Shao, Liao Xi, Heng Zhang, and Jie Zhang, "Millimeter-Wave Propagation Measurement and Modeling in Indoor Corridor and Stairwell at 26 and 38 GHz," IEEE Access, Vol. 9, pp. 87792-87805, May 2021.

[13] Muhammmad brata, and Irma Zakia, "Path Loss Estimation of 5G Millimeter WavePropagation Channel – Literature Survey," 2021 7th International Conference on Wireless and Telematics (ICWT), pp. 1-4, Aug. 2021.

[14] George R. MacCartney Jr., Sijia Deng, and Theodore S. Rappaport, "Indoor Office Plan Environment and Layout-Based MmWave Path Loss Models for 28 GHz and 73 GHz," 2016 IEEE 83rd Vehicular Technology Conference (VTC Spring), pp. 1-6, May 2016.

[15] Ahmed M. Al-samman, Tharek Abd Rahman, and Marwan Hadri Azmi, "Indoor Corridor Wideband Radio Propagation Measurements and Channel Models for 5G Millimeter Wave Wireless Communications at 19 GHz, 28 GHz, and 38 GHz Bands," Wireless Communications and Mobile Computing, Vol. 2018, Mar. 2018.

[16] Ahmed Al-Saman , Marshed Mohamed, and Michael Cheffena, "Radio Propagation Measurements in the Indoor Stairwell Environment at 3.5 and 28 GHz for 5G Wireless Networks," International Journal of Antennas and Propagation, Vol. 2020, Dec. 2020.

조선대학교
CHOSUN UNIVERSITY

[17] Pan Tang, Jianhua Zhang, Haoyu Tian, Zhaowei Chang1, Jun Men, Yuxiang Zhang, Lei Tian, Liang Xia, and Qixing Wang and Jingsuo He, “Channel Measurement and Path Loss Modeling from 220 GHz to 330 GHz for 6G Wireless Communications,” China Communications, Vol. 18, No. 5, pp. 19-32, May 2021.

[18] Jia He, Yi Chen, Yiqin Wang, Ziming Yu1, and Chong Han, “Channel Measurement and Path-Loss Characterization for Low-Terahertz Indoor Scenarios,” 2021 IEEE International Conference on Communications Workshops (ICC Workshops), pp. 1-6, Jul. 2021.

[19] Jingyuan Qian, Yating Wu, Asad Saleem, and Guoxin Zheng, “Path Loss Model for 3.5 GHz and 5.6 GHz Bands in Cascaded Tunnel Environments,” Sensors, Vol. 22, No. 12, Jun. 2022.

[20] Ahmed M. Al-Samman, Marwan Hadri Azmi, Y. A. Al-Gumaei, Tawfik Al-Hadhrami, Tharek Abd. Rahman, Yousef Fazea, and Abdulmajid Al-Mqdashi, “Millimeter Wave Propagation Measurements and Characteristics for 5G System,” Applied Sciences, Vol. 10, No. 1, Jan. 2020.